Imaging and controlling multielectron dynamics by laser-induced tunnel ionization

2011 J. Phys. B: At. Mol. Opt. Phys. 44 041001

(http://iopscience.iop.org/0953-4075/44/4/041001)

IOP PUBLISHING
IOP FTC
JOURNAL OF PHYSICS B: ATOMIC, MOLECULAR AND OPTICAL PHYSICS
J. Phys. B: At. Mol. Opt. Phys. **44** (2011) 041001 (6pp)
doi:10.1088/0953-4075/44/4/041001

FAST TRACK COMMUNICATION

Imaging and controlling multielectron dynamics by laser-induced tunnel ionization

H J Wörner[1,2] **and P B Corkum**[1]

[1] Joint Laboratory for Attosecond Science, National Research Council of Canada and University of Ottawa, 100 Sussex Drive, Ottawa, ON K1A 0R6, Canada
[2] Laboratorium für Physikalische Chemie, ETH Zürich, Wolfgang-Pauli-Strasse 10, 8093 Zürich, Switzerland

E-mail: woerner@phys.chem.ethz.ch

Received 30 November 2010, in final form 22 December 2010
Published 28 January 2011
Online at stacks.iop.org/JPhysB/44/041001

Abstract
Using sequential strong-field double ionization in a pump–probe scheme we show through calculations how electronic dynamics can be prepared and imaged. Electronic dynamics may arise whenever multiple states of the ion are accessed in the ionization step. The dynamics in the cation influence the rate of the second ionization step and the momentum distribution of the ejected electron, allowing their detailed characterization. We show how the probe step is controlled through spatial propensities of the ionizing orbitals and the energy level structure of the dication. Both the final electronic state of the dication and the spin state of the ejected electron pair can be controlled through the time delay between the two ionizing pulses. We discuss how our results will extend to the preparation and measurement of attosecond electron dynamics.

(Some figures in this article are in colour only in the electronic version)

Understanding and controlling the collective dynamics of electrons in molecules and solids is one of the central challenges of modern ultrafast science. Recent efforts have concentrated on the development of methods for the measurement of the electronic dynamics in the valence shell of atoms, molecules and solids [1–3]. This insight is expected to have important consequences for our understanding of all physical phenomena determined by the interactions between these electrons, ranging from the basic electronic structure of matter to coherent phenomena in large molecules and cooperative phenomena in solids, like supraconductivity.

An attractive approach to studying the properties of a complex system consists in removing it from equilibrium and investigating the induced dynamics. In the case of a multielectron system such a possibility is offered by temporally confined ionization [4]. The temporal confinement makes a broad bandwidth of ionic states accessible. The ensuing dynamics allows the investigation of the properties of the initial wavefunction and of the interactions of its constituents.

Strong-field ionization (SFI) in the tunnelling limit represents an attractive approach to studying and controlling the dynamics of multielectron systems. SFI usually affects multiple electronic shells implying that the ion can be left in different electronic states [5, 6]. The high nonlinearity of the strong-field interaction generates a photoelectron with a very large bandwidth, spanning tens of electron volts under typical experimental conditions. Therefore, SFI may leave the ion in a partially coherent non-stationary state [5, 7]. SFI therefore typically induces collective electron dynamics. In molecules, SFI also prepares vibrational wave packets whenever the potential surfaces of the neutral and ionic states differ [8–11].

In this communication, we show by calculations how an electronic wave packet can be imaged using SFI and used to

control the products of a subsequent ionization step. SFI is known to be highly sensitive to the electronic structure [12–14] because of its pronounced sensitivity to the shape of the ionizing orbitals. We transfer these concepts from static systems to probing electronic dynamics in atoms and molecules. As an example we use the neon atom, in which SFI prepares a spin–orbit wave packet [7, 15]. The ground state of the neon cation has two fine-structure components that are separated by 0.1 eV due to spin–orbit interaction. In this case, spin–orbit interaction drives the electronic dynamics in the cation. In virtually all polyatomic molecules, the relaxation of the orbitals upon ionization induces attosecond electronic dynamics driven by electron correlation [16, 17] which may be probed using a second ionization step, in analogy to the case discussed in this communication.

As a second aspect, we show how the proposed pump–probe experiment enables a high degree of control over the accessed state of the dication and the ejected electron pair. The dication can be prepared preferentially in either the triplet ground state or in the low-lying singlet states. Through the conservation of total spin, the ionized pair of electrons can therefore be prepared preferentially in the singlet or triplet state. Although we show model calculations for the rare gas atoms only, the underlying principles are directly applicable to all atoms and molecules possessing a fully occupied degenerate highest occupied orbital (e.g. halogen dimers, hydrogen halides, carbon dioxide, allene, benzene, etc). The ionization of these neutral species prepares a spin–orbit wave packet in the cation that can be imaged through a second ionization step.

We consider the sequential double ionization of a rare gas atom by a pair of intense (10^{14}–10^{16} W cm^{-2}) femtosecond infrared laser pulses as illustrated in figure 1. The atom (Ne, Ar, Kr or Xe) is initially in its ground electronic state $^1S_0$ of configuration $(...)(ns)^2(np)^6$. The first pulse ionizes the neutral atom almost exclusively from the p orbital aligned along the polarization of the laser pulse because the SFI rate $\Gamma_{\ell,m}$ is highly sensitive to the angular momentum projection quantum number m of the ionizing orbital [18]. As an example, the relative ionization rates of the orbital aligned along the direction of the laser field $m = 0$ to that of the perpendicular orbitals $m = \pm 1$ amounts to $\Gamma_{\ell=1,m=0}/\Gamma_{\ell=1,m=\pm1} \approx 30$ for a neon atom in a laser field of 5×10^{14} W cm^{-2}. Consequently, SFI prepares the rare gas cation in an electronic state of configuration $(...)(ns)^2(np_0^1p_{-1}^2p_{+1}^2)$, i.e. it generates an electron "hole" that is aligned along the laser field [15, 19, 20]. The corresponding wavefunction density is represented in figure 1 for $\Delta t = 0$. However, this electronic configuration does not correspond to an eigenstate of the cation, but rather to a linear combination of its two lowest spin–orbit levels:

$$\phi(t=0) = \Phi_{1,0,+1/2} = \sqrt{\frac{2}{3}}\Psi_{3/2,1/2} - \sqrt{\frac{1}{3}}\Psi_{1/2,1/2}. \quad (1)$$

The one-electron wavefunction of the missing electron has been represented in a space-fixed basis of atomic orbitals with the notation Φ_{ℓ,m,m_s}, where ℓ is the orbital angular momentum quantum number, and m and m_s are the orbital and spin angular momentum projection quantum numbers, respectively. This

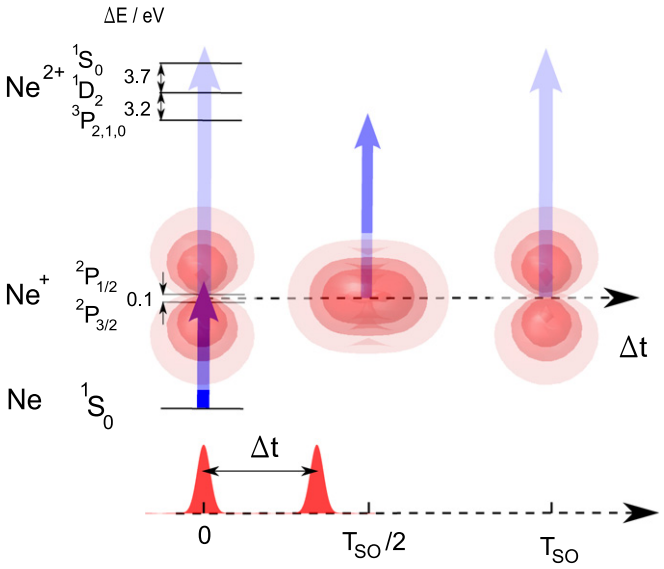

Figure 1. Illustration of the proposed pump–probe experiment. A neon atom is strong-field ionized using a few-fs infrared laser pulse, preparing Ne^+ in a coherent superposition of its two lowest fine structure levels. The electron hole subsequently rearranges between the atomic p orbitals, as illustrated through the red contour plots of its density at different time delays. A second delayed infrared laser pulse ionizes Ne^+ to Ne^{2+}. The second ionization step is suppressed at integer multiples of the wave-packet period because ionization accesses the excited singlet states of Ne^{2+}.

wavefunction is not an eigenstate of the ion when spin–orbit coupling is taken into account. However, it can be expanded into the eigenstates of the ion with the notation Ψ_{J,m_J}, where J is the total angular momentum quantum number and m_J is its projection quantum number.

This non-stationary state evolves in time according to [21]

$$\begin{aligned}\phi(t) &= \sqrt{\frac{2}{3}}e^{-i\omega_{3/2}t}\Psi_{3/2,1/2} - \sqrt{\frac{1}{3}}e^{-i\omega_{1/2}t}\Psi_{1/2,1/2} \\ &= \frac{\sqrt{2}}{3}(e^{-i\omega_{3/2}t} - e^{-i\omega_{1/2}t})\Phi_{1,1,-1/2} \\ &\quad + \left(\frac{2}{3}e^{-i\omega_{3/2}t} + \frac{1}{3}e^{-i\omega_{1/2}t}\right)\Phi_{1,0,+1/2}, \end{aligned} \quad (2)$$

where $\Delta\omega = \omega_{1/2} - \omega_{3/2}$ is related to the energetic separation ΔE_{SO} of the $^2P_{3/2}$ and $^2P_{1/2}$ states through the relation $\Delta\omega = \Delta E_{SO}/\hbar$. Ionization to $\Phi_{1,0,-1/2}$ results in a similar expression where $\Phi_{1,1,-1/2}$ and $\Phi_{1,0,+1/2}$ are replaced by $\Phi_{1,-1,+1/2}$ and $\Phi_{1,0,-1/2}$, respectively. From these formulae, the population dynamics of the hole in the space-fixed basis can be derived [21]:

$$\begin{aligned} P_{m=0} &= \tfrac{5}{9} + \tfrac{4}{9}\cos(\Delta\omega t) \\ P_{|m|=1} &= \tfrac{4}{9}(1 - \cos(\Delta\omega t)). \end{aligned} \quad (3)$$

Consequently, the population of the hole oscillates between the $m = 0$ and the $|m| = 1$ orbitals with the period $T_{SO} = h/\Delta E_{SO}$ (42.7 fs in Ne^+). In reality the coefficients of the two spin–orbit states in the coherent superposition differ slightly from those in equation (1) because of the energetic separation of the final ionic states which results in slightly

different ionization rates for the two channels. Quantitative calculations have been presented in [7] which validate our simplified model.

Since SFI is highly sensitive to the electronic structure of the ionizing orbitals, the wave packet motion will modulate the probability of a second ionization step. Two parameters affect the ionization rate of the evolving wave packet: the geometry of the ionized orbital and the energetic separation from the final states, i.e. the ionization energies of the accessible states of the dication. Ionization from an orbital aligned with the field is favoured over ionization from a perpendicular orbital. We calculate ionization rates connecting specific electronic configurations expressed in the space-fixed basis, since simple analytical formulae are available [22]. We neglect the interaction with the magnetic field of the laser pulses throughout this communication. The electronic wavefunction of the cation at any time is a linear combination of the two (np^5) configurations

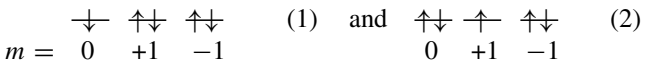

(4)

Removing one of the five electrons leads to an electronic configuration of Ne^{2+} that we resolve in the basis of electronic eigenstates using angular momentum algebra [23]:

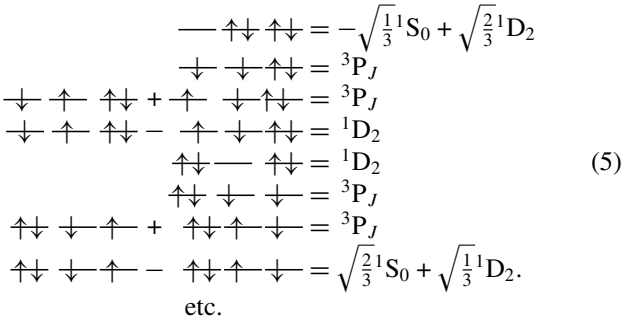

(5)

The relevant electronic states of Ne^{2+}, i.e. ^3P_J, $^1D_2$ and $^1S_0$, and their energetic separations are indicated in figure 1. We neglect the small energy splittings of the ^3P_J levels and calculate ionization rates using a kinetic model based on the tunnel ionization rates of the orbitals and their time-dependent occupation amplitude. We calculate the ionization rate of configurations (1) and (2) as a sum of all possible ionization pathways and weight them according to the population of each configuration. The ionization rate of Ne^+ in a coherent superposition state is thus given by

$$\Gamma(\Delta t) = \sum_{i=1-5}\sum_{j=1-3} P_{m=0}(\Delta t)|c_{ij}|^2\Gamma_{ij} + P_{|m|=1}(\Delta t)|c_{ij}|^2\Gamma_{ij}, \quad (6)$$

where the outer sum runs over the five valence electrons that can be removed during ionization, and the inner sum runs over the accessible electronic states of the dication. The c_{ij} are the expansion coefficients of the electronic configuration accessed by tunnel ionization into the set of electronic states given in equation (5). Γ_{ij} is the tunnel-ionization rate for removing electron i and accessing the electronic state j of the dication (^3P_J,$^1D_2$ or $^1S_0$).

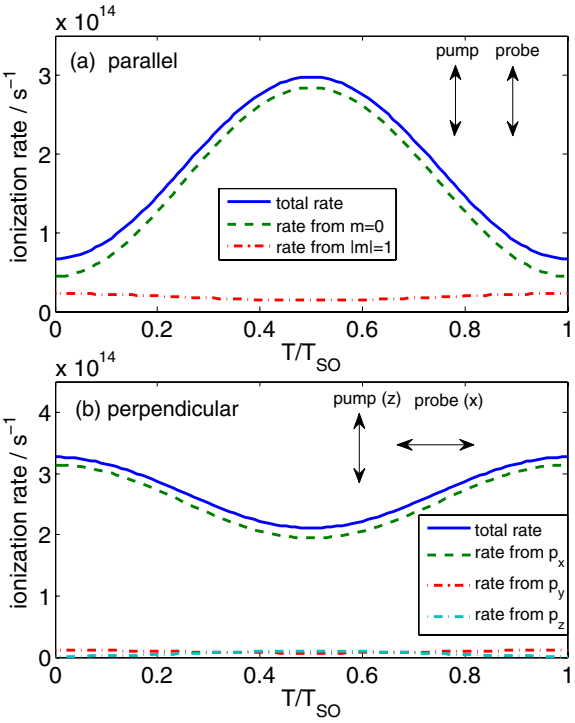

Figure 2. Calculated ionization rates of Ne^+ at an intensity of 5×10^{15} W cm^{-2} as a function of the delay after the first ionization pulse for the case of a probe pulse polarized parallel (a) or perpendicular (b) to the pump pulse. The full lines represent the total ionization rates and the broken lines represent the partial rates coming from individual orbitals. Panel (a) shows partial ionization rates from $m = 0$ (dashed line) and $m = \pm 1$ (dashed-dotted line). Panel (b) shows partial rates from all three p orbitals since they are no longer equivalent in this geometry.

We first consider the case of parallel polarizations of pump and probe laser fields. The calculated double ion yield as a function of the delay between the two laser pulses is represented in figure 2(a). The total double ion yield (full line) is found to peak at delays corresponding to half-integer multiples of the wave packet (spin–orbit) period. A decomposition of the total yield into the partial yields from the $m = 0$ and $m = \pm 1$ orbitals (dashed and dashed-dotted lines, respectively) shows that the modulation is dominated by the contribution from the $m = 0$ orbital. At half-integer multiples of the period, the hole that was created by tunnel ionization in $m = 0$ has moved to the $m = \pm 1$ orbitals according to equation (3). Thus, the population of the $m = 0$ orbital has increased from 1 to 1+8/9. Based on this effect alone, we would expect a modulation of ~ 2 in the ionization yield. The calculation however shows a modulation of the $m = 0$ yield of 6.4 (peak/valley). This is higher than what the population dynamics alone can explain. The higher modulation depth arises because the accessibility of the ionic states also varies in time as the occupation of the orbitals changes. At integer multiples of the delay, the hole is located in the $m = 0$ orbital. Thus, the second ionization step is suppressed, because removing the second electron from the $m = 0$ orbital necessarily leads to the singlet states of the cation that lie more than 3 eV above the triplet ground state. This principle is analogous to Koopman's correlations

in single-photon ionization and should be generally observable in SFI.

Figure 2(b) shows the case of perpendicularly polarized pump and probe pulses. The ionization pulse is polarized in the vertical direction (z) and thus still prepares a wave packet as shown in figure 1. The probe step preferentially removes an electron from the p_x orbital lying along its polarization direction (x). At integer multiples of the spin–orbit period, ionization from p_x leaves the dication in its ^3P_J ground state and is favoured by the double occupancy of the orbital. At half-integer multiples of T_{SO} the population of p_x decreases to 3/2, explaining that the ionization rate decreases. The modulation depth of the ionization rate from p_x is 1.6 (peak/valley), again larger than the ratio 4/3 expected from the population dynamics. This effect also results from the accessibility of the dication states.

The electronic dynamics triggered by the first ionization step should also be reflected in the momentum distributions of the electron removed in the second ionization step. Having calculated the time-dependent ionization yields of the orbitals, we now predict the momentum distributions of the second electron using a very simple model. It has been shown in [14, 24] that the continuum electron wave packet in the direction perpendicular to the ionizing laser field is well approximated by the bound momentum space orbital Ψ_b (i.e. the Fourier transform of the spatial orbital) filtered by a Gaussian function that accounts for the suppression of large linear momenta in the tunnelling process:

$$\Psi_{c,\perp} = \Psi_{b,\perp} \exp\left(-\frac{\sqrt{I_p}}{\sqrt{2}E} p_\perp^2\right), \qquad (7)$$

where E is the laser electric field amplitude and $p_\perp$ is the perpendicular component of the electron momentum.

Using the calculated temporal evolution of the partial ionization rates, we can thus predict the time-dependent shape of the electron momentum distribution as

$$D_\perp(\Delta t) = \Gamma_{m=0}(\Delta t) D_{\perp,m=0} + \Gamma_{|m|=1}(\Delta t) D_{\perp,|m|=1}, \qquad (8)$$

where $D_{\perp,m} = |\Psi_{c,\perp,m}|^2$ is the momentum distribution obtained from ionization of a p_m orbital of Ne^+. Figure 3 shows the calculated lateral electron momentum distributions for ionization of Ne^+ at time delays nT_{SO} (a) and $[(2n+1)/2]T_{SO}$ (b). The full lines represent the total distribution and the dashed and dashed-dotted lines represent the contributions from the $m = 0$ and $|m| = 1$ orbitals, respectively. As a result of the cylindrical symmetry in the case of parallel pump and probe polarizations, the electron momentum distributions have circular symmetry and are fully characterized by a one-dimensional cut through the origin. (a) At integer multiples of the wave-packet period the momentum distribution is broad, since $m = 0$ and $m = 1$ orbitals contribute with comparable importance. (b) At half-integer multiples of the delay the distribution becomes narrower as the ionization from the $m = 0$ orbital dominates.

So far, we have shown how electronic dynamics induced by the first ionization step can be probed and imaged using the second step. Every pump–probe experiment also offers an opportunity for quantum control which is particularly

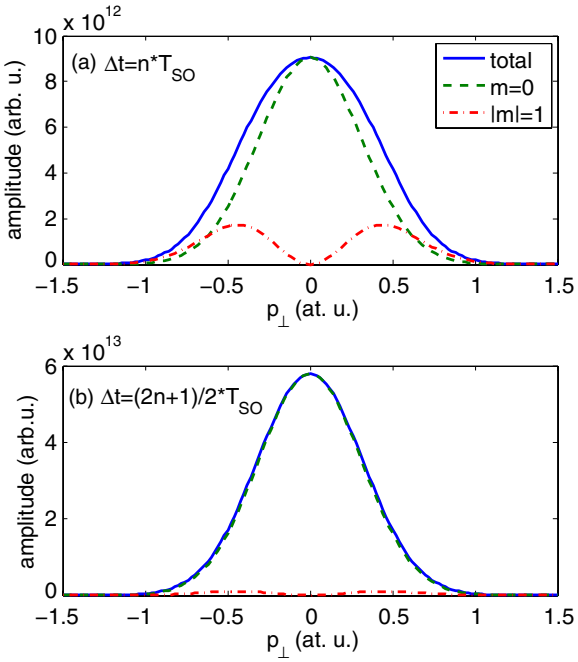

Figure 3. Calculated lateral momentum distribution of electrons tunnel ionized by a laser field of intensity 5×10^{15} W cm^{-2} from Ne^+ at delays Δt after the pump pulse. At delays corresponding to integer multiples of the spin–orbit period, ionization from $|m| = 1$ significantly contributes to and broadens the total electron distribution as shown in panel (a). At half-integer delays, ionization from $m = 0$ dominates, resulting in a narrower momentum distribution.

interesting in the present case. We have shown how the occupation of orbitals affects the accessible states of the dication. At half-integer multiples of the wave-packet period, the ^3P_J ground state of the dication is accessible through the preferred ionization from $m = 0$ and is thus the main product of the second ionization step. At integer multiples of the period, the ^3P_J states are only accessible through $|m| = 1$ ionization, whereas the $^1D_2$ and $^1S_0$ states are accessible through $m = 0$ ionization—at the cost of a higher ionization energy. This results in a preferred ionization into the singlet states.

The time-dependent yield of Ne^{2+} in triplet or singlet states is represented in figure 4. The full line represents the total yield of Ne^{2+} which is identical to that shown in figure 2(a). The dashed and dashed-dotted lines represent the partial yields of Ne^{2+} in one of the ^3P_J or one of the singlet ($^1D_2$,$^1S_0$) states, respectively. In addition to the electronic state of the cation, the spin state of the ejected electron pair can also be controlled. Total spin has to be conserved as long as the interaction with the magnetic field of the laser pulses can be neglected. This situation applies for moderate intensities below 10^{16} W cm^{-2}. Thus, control over the final state of the dication implies control over the spin state of the electron pair. It is therefore possible to control the entanglement of the electrons ejected in sequential double ionization.

In conclusion, we have shown that sequential SFI by a pair of ultrashort infrared laser pulses can be used to image electronic dynamics initiated by the first laser

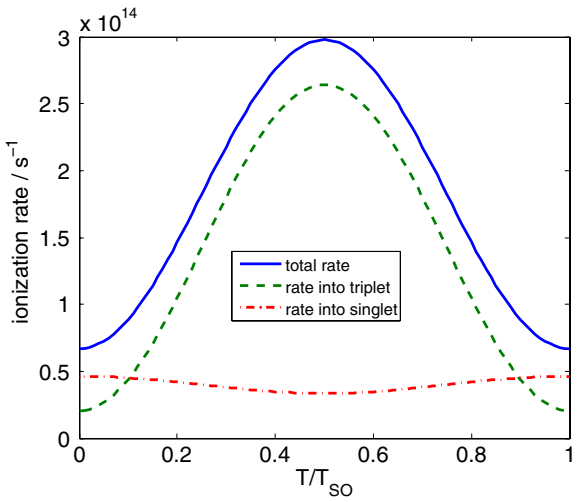

Figure 4. Calculated ionization rate of Ne^+ at an intensity of 5×10^{15} W cm^{-2} as a function of the delay after the first ionization pulse for parallel polarizations of pump and probe pulses. The full line shows the total ionization rate which is the same as in figure 2(a). The dashed line represents ionization into the ^3P_J ground state of Ne^{2+} which is accompanied by the formation of an electron pair in a triplet state. The dashed-dotted line represents ionization to the $^1D_2$ or $^1S_0$ state of Ne^{2+} and the formation of a singlet electron pair.

pulse. Using the rare gas atoms as an example, we have shown how electronic dynamics influences the ionization rate and momentum distributions of the second ionization step. Spin–orbit dynamics in neon and argon will be readily accessible using 800 nm pulses of less than 10 fs [15]. In krypton and xenon, the spin–orbit dynamics is faster (6.2 and 3.2 fs, respectively). As pointed out in [7], this leads to a low degree of coherence after the ionization pulse because the optical cycle period is incommensurate with the electronic dynamics. This limitation can be overcome by using even shorter laser pulses in which a single optical cycle dominates [3] or by synchronizing the optical cycle period to the electronic dynamics that is being prepared. For example, when xenon is tunnel ionized in a laser field of wavelength 1900 nm, the half-cycle period matches the internal dynamics of Xe^+ which allows the preparation of a highly coherent state even in a multicycle pulse. A pair of such pulses could then be used to perform the measurements described in this communication. Such an experiment would be a highly nonlinear variant of the classical Ramsey fringe experiment.

Looking forward, it appears that SFI will become an attractive method to prepare attosecond dynamics. The nonlinearity of the process enforces temporal confinement which results in the formation of the ion in a coherent superposition of multiple electronic states. Therefore, attosecond electronic dynamics can be readily prepared. We have used spin–orbit dynamics to illustrate a general phenomenon: after ionization the cation is usually in a non-stationary state [4]. Electron correlation drives the rearrangement of the electronic structure of the ionized system, providing access to their characterization. The most general method for probing these dynamics will use an isolated attosecond pulse in combination with either photoelectron detection [25] or transient absorption [26].

Acknowledgments

We thank David Villeneuve, André Staudte and Avner Fleischer for discussions. HJW acknowledges support from the Swiss National Science Foundation under grant PP00P2_128274.

Note added: The method proposed in this communication has recently been realized experimentally and extended to molecules [27].

References

[1] Uiberacker M *et al* 2007 Attosecond real-time observation of electron tunnelling in atoms *Nature* **446** 627
[2] Cavalieri A L *et al* 2007 Attosecond spectroscopy in condensed matter *Nature* **449** 1029
[3] Goulielmakis E *et al* 2008 Single-cycle nonlinear optics *Science* **320** 1614
[4] Breidbach J and Cederbaum L S 2005 Universal attosecond response to the removal of an electron *Phys. Rev. Lett.* **94** 033901
[5] Smirnova O, Mairesse Y, Patchkovskii S, Dudovich N, Villeneuve D M, Corkum P B and Ivanov M Yu 2009 High harmonic interferometry of multi-electron dynamics in molecules *Nature* **460** 972
[6] McFarland B K, Farrell J P, Bucksbaum P H and Gühr M 2008 High-harmonic generation from multiple orbitals N_2 *Science* **322** 1232
[7] Rohringer N and Santra R 2009 Multichannel coherence in strong-field ionization *Phys. Rev.* A **79** 053402
[8] Niikura H, Légaré F, Hasbani R, Bandrauk A D, Ivanov Yu M, Villeneuve D M and Corkum P B 2002 Sub-laser-cycle electron pulses for probing molecular dynamics *Nature* **417** 917
[9] Baker S, Robinson J S, Haworth C A, Teng H, Smith R A, Chirila C C, Lein M, Tisch J W G and Marangos J P 2006 Probing proton dynamics in molecules on an attosecond time scale *Science* **312** 424
[10] Ergler Th, Rudenko A, Feuerstein B, Zrost K, Schröter C D, Moshammer R and Ullrich J 2006 Spatiotemporal imaging of ultrafast molecular motion: collapse and revival of the D_2^+ nuclear wave packet *Phys. Rev. Lett.* **97** 193001
[11] Fang L and Gibson G N 2007 Investigating excited electronic states of I_2^+ and I_2^{2+} produced by strong-field ionization using vibrational wave packets *Phys. Rev.* A **75** 063410
[12] Muth-Böhm J, Becker A and Faisal F H M 2000 Suppressed molecular ionization for a class of diatomics in intense femtosecond laser fields *Phys. Rev. Lett.* **85** 2280
[13] Pavičić D, Lee K F, Rayner D M, Corkum P B and Villeneuve D M 2007 Direct measurement of the angular dependence of ionization for N_2, O_2, and CO_2 in intense laser fields *Phys. Rev. Lett.* **98** 243001
[14] Meckel M *et al* 2008 Laser induced electron tunnelling and diffraction *Science* **320** 1478
[15] Santra R, Dunford R W and Young L 2006 Spin-orbit effect on strong-field ionization of krypton *Phys. Rev.* A **74** 043403
[16] Breidbach J and Cederbaum L S 2003 Migration of holes: formalism, mechanisms and illustrative applications *J. Chem. Phys.* **118** 3983
[17] Remacle F and Levine R D 2006 An electronic time scale in chemistry *Proc. Natl Acad. Sci. USA* **103** 6793

[18] Otobe T, Yabana K and Iwata J I 2004 First-principles calculations for the tunnel ionization rate of atoms and molecules *Phys. Rev.* A **69** 053404
[19] Young L *et al* 2006 X-ray microprobe of orbital alignment in strong-field ionized atoms *Phys. Rev. Lett.* **97** 083601
[20] Loh Z H, Kahil M, Correa R E, Santra R, Buth Ch and Leone S R 2007 Quantum state-resolved probing of strong-field-ionized xenon atoms using femtosecond high-order harmonic transient absorption spectroscopy *Phys. Rev. Lett.* **98** 143601
[21] Wen H, Pisharody S N, Murray J M and Bucksbaum P H 2006 Observing angular precession of a Rydberg wave packet due to spin–orbit coupling by orthogonally polarized weak half-cycle pulses *Phys. Rev.* A **73** 052504
[22] Yudin G L and Ivanov M Yu 2001 Nonadiabatic tunnel ionization: looking inside a laser cycle *Phys. Rev.* A **64** 013409
[23] Zare R N 1988 *Angular Momentum* (New York: Wiley)
[24] Spanner M, Simova O, Corkum P B and Ivanov M Yu 2004 Reading diffraction images in strong field ionization of diatomic molecules *J. Phys. B: At. Mol. Opt. Phys.* **37** L243
[25] Kienberger R *et al* 2003 Atomic transient recorder *Nature* **427** 817
[26] Goulielmakis E *et al* 2010 Real-time observation of valence electron motion *Nature* **466** 739
[27] Fleischer A, Wörner H J, Arissian L, Liu L R, Meckel M, Rippert A, Dörner R, Villeneuve D M, Staudte A and Corkum P B Probing electron correlations by laser-induced tunnel ionization *Nature* submitted